Shunqi Xu, Yungui Li, Bishnu P. Biswal, Matthew A. Addicoat, Silvia Paasch, Paulius Imbrasas, SangWook Park, Huanhuan Shi, Eike Brunner, Marcus Richter, Simone Lenk, Sebastian Reineke, Xinliang Feng

Luminescent sp2-Carbon-Linked 2D Conjugated Polymers with High Photostability

Erstveröffentlichung in / First published in:

Chemistry of Materials. 2020, 32(18), S. 7985–7991. ISSN 1520-5002.

DOI: https://doi.org/10.1021/acs.chemmater.0c02910

Luminescent sp^2-Carbon-Linked 2D Conjugated Polymers with High Photostability

Shunqi Xu,[†#] Yungui Li, [‡#] Bishnu P. Biswal,[†&] Matthew A. Addicoat,[‖] Silvia Paasch,[§] Paulius Imbrasas,[‡] SangWook Park,[†] Huanhuan Shi,[†] Eike Brunner,[§] Marcus Richter,[†] Simone Lenk,[‡] Sebastian Reineke,[‡*] Xinliang Feng[†*]

[†] Technische Universität Dresden, Center for Advancing Electronics Dresden (cfaed) and Faculty of Chemistry and Food Chemistry, Chair of Molecular Functional Materials, Mommsenstraße 4, 01069 Dresden (Germany)
[‡] Technische Universität Dresden, Dresden Integrated Center for Applied Physics and Photonic Materials (IAPP), Chair for Organic Semiconductors, Nöthnitzer Straße 61, 01069 Dresden (Germany)
[‖] Nottingham Trent University Clifton Lane, School of Science and Technology, Nottingham, NG118NS (United Kingdom)
[§] Technische Universität Dresden, Department of Chemistry and Food Chemistry, Chair of Bioanalytical Chemistry, Bergstraße 66, 01069 Dresden (Germany)

ABSTRACT: Luminescent organic materials with high photostability are essential in optoelectronics, sensor, and photocatalysis applications. However, small organic molecules are generally sensitive to UV irradiation, giving rise to chemical decompositions. In this work, we demonstrate two novel CN-substituted two-dimensional sp^2-carbon-linked conjugated polymers (2D CCPs) containing a chromophore triphenylene unit. The Knoevenagel polymerization between 2,3,6,7,10,11-hexakis(4-formylphenyl)triphenylene (HFPTP) and 1,4-phenylenediacetonitrile (PDAN) or 2,2'-(biphenyl-4,4'-diyl)diacetonitrile (BDAN), provides the crystalline 2D CCP-HFPTP-PDAN (2D CCP-1) and 2D CCP-HFPTP-BDAN (2D CCP-2) with dual pore structures, respectively. 2D CCP-1 and 2D CCP-2 exhibit the photoluminescence quantum yield (PLQY) up to 24.9% and 32.3%, which are the highest values among the reported 2D conjugated polymers and π-conjugated 2D covalent organic frameworks. Furthermore, compared with the well-known emissive small molecule tetrakis(carbazol-9-yl)-4,6-dicyanobenzene (4CzIPN), both 2D CCPs show superior photostability under UV irradiation for two hours, profiting from the twisted and rigid structures of the CN-substituted vinylene linkages. The present work will trigger the further explorations of novel organic emitters embedded in 2D CCPs with high PLQY and photostability, which can be useful for optoelectronic devices.

Organic emissive materials play a crucial role in applications such as lighting, sensing and bio-imaging.[1–4] Compared to inorganic or hybrid perovskite emitters, purely organic emitters are environmental-friendly without hazardous ingredients.[5] They have the advantages of design flexibility and color tunability in a broad span of wavelengths. The continuous development of organic emitters has facilitated the tremendous technological progress of organic light-emitting diodes and organic lasers.[4,6,7] However, for conventional organic emitting small molecules, dendrimers and polymers, some chemical bonds with low energies such as C-H (3.6~4.2 eV) and C-N (3.16 eV) can lead to photobleaching under UV radiation, which hinders their applications in the circumstances with the presence of oxygen and UV excitation.[8–10] Clearly, the development of emissive organic materials with high photostability is of utmost importance for applications such as in light sensing and bio-imaging.[1-4]

Two-dimensional (2D) conjugated polymers, also classified as 2D π-conjugated covalent organic frameworks (COFs), are crystalline porous polymers with π-extended conjugation and tailorable topologies and lattice structures of repeating units.[11–15] These materials have drawn increasing attention due to their predictable structures and tunable optoelectronic properties by the organic synthesis.[11–16] In particular, with delicate design, 2D conjugated polymers can restrict the rotational/vibrational relaxation for robust solid emissive materials.[12,16] So far, 2D conjugated polymers have been mostly synthesized via the dynamic imine chemistries.[11-12] However, the thermal dissipation resulting from the rotationally labile imine bonds (**Figure 1c)** and the aggregation-caused quenching (ACQ) induced by the π–π stacking between the layered conjugated structures can easily lead to tremendous emission quenching under photoexcitation, which has impeded the development of 2D conjugated polymers as robust emissive materials.[12,16] In this respect, cyano-substituted 2D sp^2-carbon-linked conjugated polymers (2D CCPs) may overcome the emission quenching issue, because the CN-substituted vinylene compound was recently reported to enable the aggregation-induced emission (AIE) effect.[17] Nevertheless, it is still of great

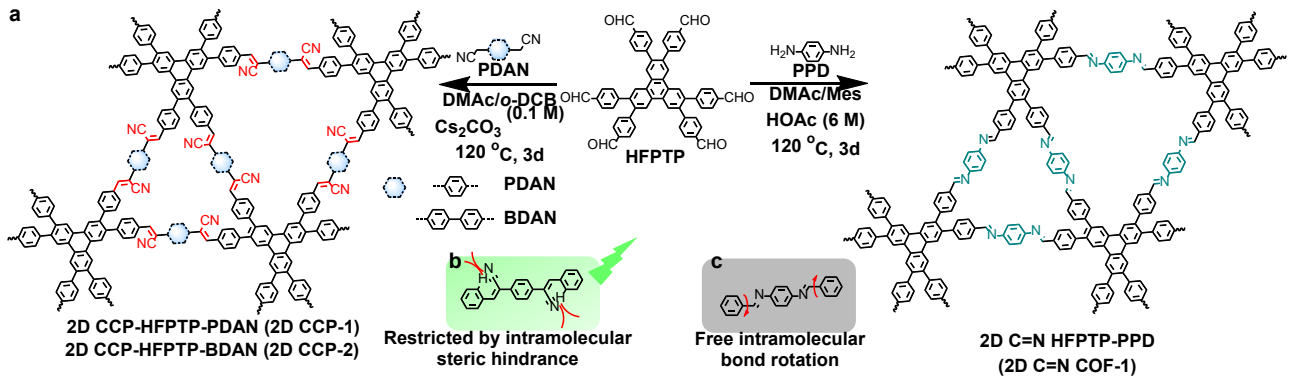

Figure 1. (a) Scheme for the synthesis of 2D CCP-1, 2D CCP-2, and 2D C=N COF-1 from HFPTP; (b) Twist and rigid [-CH=C(CN)-] linkage induce solid-state emission; (c) Intramolecular rotation of imine linkages quenches the emission.

challenge to develop the CN-substituted 2D CCPs with strong solid-state emission,[18,19] and the photostability of such materials remains unexplored.

In this work, we demonstrated two novel CN-substituted 2D CCPs via the Knoevenagel polymerization between 2,3,6,7,10,11-hexakis(4-formylphenyl)triphenylene (HFPTP) and 1,4-phenylenediacetonitrile (PDAN) or 2,2'-(biphenyl-4,4'-diyl)diacetonitrile (BDAN), providing 2D CCP-HFPTP-PDAN (2D CCP-1) and 2D CCP-HFPTP-BDAN (2D CCP-2) (**Figure 1a**), respectively. Together with the corresponding imine-linked 2D COF (2D C=N HFPTP-PPD, also named as 2D C=N COF-1), powder x-ray diffraction (PXRD) patterns, and the N_2 adsorption-desorption measurements confirm the formation of crystalline 2D CCPs with a dual-pore structure. Remarkably, the solid 2D CCP-1 shows a high PLQY of 24.9%, which is 60 times higher than the corresponding imine-linked 2D COF. Moreover, the solid 2D CCP-2 exhibits a high PLQY of 32.3%. To the best of our knowledge, the PLQYs of both 2D CCPs in this work are the highest values among all the reported 2D conjugated polymers and π-conjugated COFs.[16,18–24] The outstanding emissive properties can be attributed to the presence of C=C-CN linkages, which can block the non-radiative molecular rotation due to the steric hindrance between the cyano groups and hydrogens on the adjacent benzene rings (**Figure 1b**),[17] and reduced ACQ effects resulting from the weak π–π stacking interactions between adjacent layers. Furthermore, both 2D CCPs present a higher photostability under UV irradiation for two hours than the well-known organic emitter tetrakis(carbazol-9-yl)-4,6-dicyanobenzene (4CzIPN).[10,25]

Experimental/Methods section

The commercial chemicals and solvents: Triphenylene, and Tetrakis(triphenylphosphine)palladium(0) [$Pd(Ph_3)_4$], Caesium carbonate (Cs_2CO_3), and 1,4-phenylenediacetonitrile (PDAN) were purchased from TCI Deutschland GmbH; the 4-Formylbenzeneboronic acid was purchased from Manchester Organics. All the solvents were purchased from Sigma Aldrich and used without any further purification. Column chromatography was done with silica gel (particle size 0.063-0.2 mm from VWR) and silica coated aluminum sheets with fluorescence indicator from Merck were used for thin layer chromatography.

Solution ^{1}H and ^{13}C NMR data were collected via a BRUKER AVANCE III 300 spectrometer at room temperature with standard pulse programs. Chemical shifts (δ) are reported in parts per million (ppm) relative to traces of [H^1] solvent in the corresponding deuterated solvent. The solvent signals were used as references ($CDCl_3$: δ(^{1}H) = 7.26 and δ (^{13}C) = 77.00 ppm).

High-Resolution (HR) Mass spectra were got on a Bruker Autoflex Speed MALDI-ToF MS (Bruker Daltonics, Bremen, Germany) with *trans*-2-[3-(4-*tert*-Butylphenyl)-2-methyl-2-propenylidene]malononitrile (DCTB) as the matrix.

Fourier transform infrared (FT-IR) spectra were recorded on a Bruker Tensor II IR spectrometer with a universal Zn-Se ATR (attenuated total reflection) accessory in the 600~4000 cm^{-1}.

^{13}C CP solid-state NMR spectra were recorded on a BRUKER Ascend 800 MHz spectrometer using a commercial 3.2 mm MAS NMR probe and operating at a resonance frequency of 201.2 MHz. The experimental NMR spectra of the three 2D conjugated polymers agree well with the predicted NMR data calculated with the program ACD/Labs.

Scanning electron microscopy (SEM) was carried out on a field emission scanning electron microscope (FESEM, Zeiss Gemini 500).

Transmission electron microscopy (TEM) was performed on a high-resolution transmission electron microscope (HRTEM, JEM-2100, JEOL, Japan). The samples were carefully prepared by dropping dispersions of 2D conjugated polymers in anhydrous ethanol onto the copper grid followed by removal of the solvent under vacuum.

Powder X-ray diffraction measurements (P-XRD) were carried out on the STOE STADI P diffractometer, using mono chromated Cu/Kα (λ = 0.1542 nm) source. The sample was pressed as a film and investigated in transmission geometry. The PXRD was carried with the parameter of 1 step with 60 s for synthesized polymer frameworks for collecting data.

The modeling of 2D conjugated polymers*:** The parameters for C, N, and H atoms were taken from the Mio-0-1 parameter set, and Lennard-Jones dispersion was employed.The Pawley refinement of the experimental PXRD*** was conducted by the Reflux module in BIOVIA Materials Studio 2017.

Nitrogen adsorption-desorption isotherm measurements were carried out using a Quadrasorb SI MP. Before gas adsorption measurements, the as-prepared samples (~50 mg) were dried under dynamic vacuum at 150 °C for 8 h. The resulting samples were then used for gas adsorption measurements from 0 to 1 atm at 77 K. The Brunauer-Emmett-Teller (BET) method was utilized to calculate the specific surface areas. By using the non-local density functional theory model, the pore volumes were derived from the sorption curves.

UV-visible absorption spectra were measured on an Agilent Cary 5000 UV-Vis-NIR spectrophotometer by using a 10 mm

optical-path quartz cell at room temperature in an integration sphere.

Lumiescene emission spectra were recorded on a Perkin Elmer LS-55.

Photoluminescent quantum yields (PLQY) and time-correlated single-photon counting (TCSPC) measurements were conducted by dispersing PMMA with 2 wt% 2D conjugated polymers in anhydrous tetrahydrofuran (THF) by ultrasonic bath for 30 min, and further spin-coated on quartz glass, which was then used for photoluminescent quantum yields (PLQY). The samples for TCSPC measurement are prepared by dip-coating. A calibrated integrating sphere in N_2 or ambient atmosphere was compared to confirm the PLQY of these films with a CAS 140 CT spectrometer and a UV-LED.[31] For transient measurements, a picosecond time-correlated single-photon counting technique was used. After exciting the sample with a laser diode head (PicoQuant LDH-D-C-375) at 375 nm with a pulse width of 44 ps, the emission was collected from a photomultiplier tube (PicoQuant PMA Hybrid) and data acquisition was handled by a TCSPC module (PicoQuant TimeHarp 260). The decay of the prompt fluorescence can be fitted by multi-exponential functions, with the following formula[32]:

$$y = \sum_i A_i \exp\left(-\frac{x}{\tau_i}\right) + y_0$$

The averaged decay lifetimes can be obtained by:

$$\tau_a = \frac{\sum_i A_i \tau_i^2}{\sum_i A_i \tau_i}$$

Photostability is investigated by putting films or powders under UV radiation for two hours. The test was done in a glovebox by a portable UV lamp with four tubes distributed evenly, each specified with 9 W electrical power. The sample is put with a distance of ~10 cm to the UV tubes.

Synthesis of 2D CCP-1**:** 1,4-phenylenediacetonitrile (PDAN, 6.59 mg, 42 μmol), HFPTP (12 mg, 14 μmol) and Cs_2CO_3 (0.1 M, 0.1 mL) were added into a mixture of *N*,*N*-dimethylacetamide (DMAc, 0.5 mL) and *ortho*-dichlorobenzene (*o*-DCB, 0.5 mL) in an ampoule. The ampoule was sealed under vacuum after three freeze-pump-thaw cycles. Afterwards, the mixture was sonicated for five mins at room temperature and then heated at 120 ºC for three days in oven. After cooling to room temperature, the precipitate was filtered and washed with DMF, water, and acetone for three times. The resulting powder was dried under vacuum at 120 ºC for three hours to afford target 2D CCP-1 as a green powder (17.5 mg, 85%).

Synthesis of 2D CCP-2**:** 2,2'-(biphenyl-4,4'-diyl)diacetonitrile (BDAN, 9.8 mg, 42 μmol), HFPTP (12 mg, 14 μmol) and Cs_2CO_3 (0.1 M, 0.1 mL) were added into a mixture of DMAc (0.5 mL) and *o*-DCB (0.5 mL) in an ampoule. The ampoule was sealed under vacuum after three freeze-pump-thaw cycles. Afterwards, the mixture was sonicated for five mins at room temperature and then heated at 120 ºC for three days in oven. After cooling to room temperature, the precipitate was filtered and washed with DMF, water, and acetone for three times. The resulting powder was dried under vacuum at 120 °C for three hours to afford the target 2D CCP-2 as a green powder (19.4 mg, 89%).

Synthesis of 2D C=N COF-1**:** *p*-phenylenediamine (PPD, 5.71 mg, 52.76 μmol) and HFPTP (15 mg, 17.59 μmol) and were added into a mixture of dimethylacetamide (DMAc, 0.5 mL), mesitylene (Mes, 0.5 mL) and acetic acid (aq. 6M. 0.1 mL) in a glass ampoule. The ampoule was sealed under vacuum after three-pump-thaw cycles. Then the mixture was sonicated for 5 mins after warmed to room temperature and heated at 120 oC for three days. After cooling to room temperature, the precipitate was filtered and washed with anhydrous N,N-dimethylformamide (DMF), dioxane, acetone for three times. Subsequently, the powder was dried under vacuum at 120 ºC for three hours to afford a green powder (15.2 mg, 73%). 2D C=N COF-1 was insoluble in the most common organic solvents, such as DMF, acetone, dichloromethane (DCM).

Results and Discussion

Both 2D CCP-1 and 2D CCP-2 were synthesized by heating triphenylene-containing building block 2,3,6,7,10,11-hexakis(4-formylphenyl)triphenylene (HFPTP, 1.0 equiv) with 1,4- phenylenediacetonitrile (PDAN) and 2,2'-(biphenyl-4,4'-diyl)diacetonitrile (BDAN), respectively, in the mixture of dimethylacetamide (DMAc)/ *ortho*-dichlorobenzene (*o*-DCB)/Cs_2CO_3 (0.1 M) =5/5/1 at 120 ºC for three days. The imine-linked 2D C=N COF-1 was synthesized by heating HFPTP (1.0 equiv) with *p*-phenylenediamine (PPD, 3.0 equiv) in the mixture of dimethylacetamide (DMAc)/mesitylene (Mes)/acetic acid (HOAc, 6 M)= 5/5/1 at 120 ºC for three days. The achieved 2D CCP-1 and 2D CCP-2 were washed with dimethylformamide (DMF), water, and acetone for three times, affording green powders with high yields of 85% and 89%, respectively. The 2D C=N COF-1 was washed with anhydrous DMF, dioxane, and acetone for three times, which provided green powder with a yield of 73%.

Fourier Transform Infrared Spectroscopy (FT-IR) and solid-state ^{13}C-NMR were conducted firstly to examine the polymerization efficiencies. As shown in **Figure S1-2**, in the FT-IR spectra of 2D CCP-1 and 2D CCP-2, the disappearance of the absorption around 2729-2823 cm^{-1} (-CHO groups) and the shift in the absorption peak from ~2245 cm^{-1}(-CN) to ~2210 cm^{-1} (-CH=C-CN) indicate the efficient polymerization (For 2D C=N COF-1, see **Figure S3**). In the solid-state ^{13}C-NMR spectra, as shown in **Figure 2a-b**, the chemical shifts of around ~118 and ~110 ppm in 2D CCP-1 and 2D CCP-2 can be assigned to the formation of the CN-substituted vinylene linkages (For 2D C=N COF-1, see **Figure S6**). Field emission scanning electron microscope (SEM) presents spherical morphology for 2D C=N COF-1 and flower-like morphology for 2D CCP-1 and 2D CCP-2, respectively (**Figure S7-9**). Transmission electron microscopy (TEM) images of all three 2D conjugated polymers unambiguously confirm the sheet structures in the nanoscale (Figure **S10-12**).

The interior architectures of the 2D CCP-1 and 2D CCP-2 were further investigated by experimental and simulated PXRD patterns. As shown in **Figure 2c-d**, the peaks at 4.11º, 7.23º, 8.17º in the experimental PXRD patterns of 2D CCP-1 and 2D C=N COF-1 (**Figure S17**) and 3.56º, 6.02º, 7.14º in the experimental PXRD patterns of 2D CCP-2, can be assigned to (100), (110) and (200), respectively, indicating the formation of long-range ordered structures in two dimensions. The 2D CCP-1 has comparable PXRD signal positions with their corresponding imine-linked analog[26] (**Figure S13**) due to their close unit cells, further suggesting the successful construction of the expected 2D CCPs. The stacking models of both 2D CCPs with eclipsed (AA) stacking, slipped AA stacking, and staggered (AB) stacking are calculated from optimized monolayer structures by density-functional tight-binding method (DFTB$^+$) and the mio-0-1

parameter set.[27] The calculations show that the slipped AA stacking models are preferable than eclipsed AA stacking and AB stacking with per-layer stabilization energies of 92.06 kcal mol^{-1} for 2D CCP-1, and 107.43 kcal mol^{-1} for 2D CCP-2, respectively. Pawley refinements based on the optimized structures are further performed using Reflex package in Accelrys's Materials Studio 7.0 software, giving the unit-cell parameters of a =25.83 Å, b = 24.95 Å, and c = 7.59 Å, and α =74.47 °, β = 80.05 ° and γ =61.51 °, with R_{wp} = 1.95 % and R_p = 1.53 % for 2D CCP-1; a=30.34 Å, b = 30.34 Å, and c = 7.25 Å, and α = 91.90 °, β = 95.16 ° and γ =60.28 °, with R_{wp} = 3.0 % and R_p = 2.36 % for 2D CCP-2, respectively (One unit cell contains two layers). The difference plots also show that the refined diffraction patterns are consistent with the corresponding experimental PXRD data.

N_2 adsorption-desorption measurements were conducted at 77 K to study their porosities. As shown in Figure **2e-f and Figure S22-23**, there is a sharp rise in the low-pressure range (P/P_0=0~0.01) in all isotherm plots, which belong to typical **I** sorption isotherm, indicating a microporous nature. The Brunauer-Emmett-Teller (BET) surface areas of 2D CCP-1, 2D CCP-2, and 2D C=N COF-1 are calculated to be 336, 102, and 575 m^2/g, respectively. The pore-size distribution based on density functional theory (NLDFT) reveals two peaks at ~0.6 and 1.3 nm for 2D CCP-1 and 2D C=N COF-1, ~1.2 and 1.9 nm for 2D CCP-2, respectively, which match very well with the theoratical values (**Figure S18**). The lower BET surface area of 2D CCPs is be attributed to a lower crystallinity compared with the imine-linked 2D COFs. Thereby, together with the above FT-IR, solid-state ^{13}C-NMR, N_2 adsorption-desorption measurement, as well as the experimental and simulated PXRD patterns, the successful formation of 2D CCP-1 and 2D CCP-2 is demonstrated.

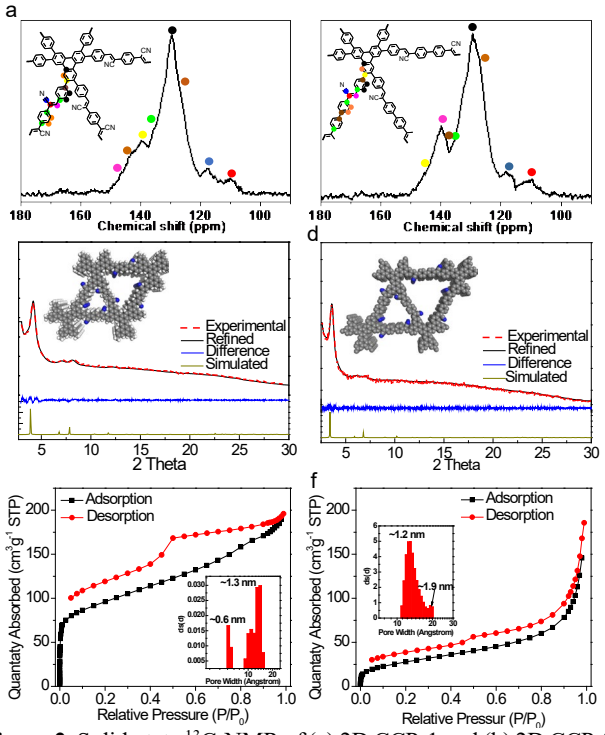

Figure 2. Solid-state ^{13}C-NMR of (a) 2D CCP-1 and (b) 2D CCP-2; Experimental (red dashed), Pawley-refined (black), simulated PXRD patterns (green) and difference plots (blue) for (c) 2D CCP-1 and (d) 2D CCP-2; N_2 adsorption-desorption isotherms and pore size distribution (inside) of (e) 2D CCP-1 and (f) 2D CCP 2.

The UV-Vis absorption spectra (**Figure 3a**) of 2D conjugated polymer dispersions in isopropanol show the absorption edge of approximately 484, 483, and 476 nm for 2D CCP-1, 2D CCP-2, and 2D C=N COF-1, respectively. The Tauc plot analysis (**Figure S24**) of the UV-Vis absorption spectrum reveals the optical bandgap of 2.66, 2.63, 2.65 eV for 2D CCP-1, 2D CCP-2, and 2D C=N COF-1, respectively. Photoluminescence (PL) spectra of the dispersions show a maxima peak at 507 nm and 500 nm for 2D CCP-1 and 2D CCP-2 (**Figure 3b**), respectively. In contrast, there is almost no apparent emission for 2D C=N COF-1 dispersion (**Figure 3b**). Afterwards, the absolute PLQY of solid 2D CCP-1 was measured as high as 24.9%,[28] which is 60 times higher than the corresponding 2D C=N COF-1 (0.4%). Furthermore the PLQY of 2D CCP-2 reaches 32.3% (**Figure 3c**). This PLQY values of the 2D CCPs can be attributed to the [-CH=C(CN)-] linkage that enhances the emission by restricting the intramolecular bond rotation (**Figure S19**), which was also observed in small molecules.[17] To the best of our knowledge, the achieved PLQYs are the highest among those of reported 2D conjugated polymers and 2D π-conjugated COFs.[16,18–24] Time-correlated single-photon counting (TCSPC) measurements revealed that the lifetime of prompt emission in N_2 for the 2D CCP-1 and 2D CCP-2 is 7.5 and 6.6 ns (**Figure 3d**), respectively. Only negligible lifetime change is observed in the ambient atmosphere, as summarized in supplementary **table S4-S5**. The lifetime fitting is presented in **SI** from Figure **S25-S30**. The temperature-dependent transient PL emission shown in Figure **S31-S32** for both 2D CCPs were then conducted to investigate their decay kinetics. When increasing the temperature from 77 K, 100 K, 150K, 200 K, 250 K, to 300 K, the emission of both 2D CCPs are identical. Compared to conventional fluorescent emitters with temperature-dependent decay kinetics, the identical transient behavior at different temperatures indicates the intrinsic rigid molecular structures in these 2D CCPs, by which the molecular rotation and temperature-dependent non-radiative decay are therefore largely suppressed.[29]

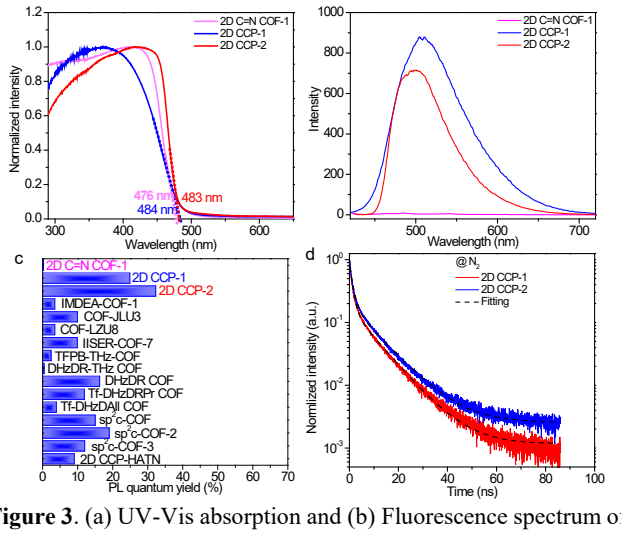

Figure 3. (a) UV-Vis absorption and (b) Fluorescence spectrum of 2D CCP-1 (blue), 2D CCP-2 (red) and 2D C=N COF-1 (pink) dispersion in isopropanol (concentration = 0.1 mg/ml). (c) PLQY of solid 2D CCP-1, 2D CCP-2, 2D C=N COF-1, and reported 2D conjugated polymers; [16,18–24] (d) The prompt luminescence curves of 2D CCP-1 (blue) and 2D CCP-2 (red) in N_2 atmosphere.

The photostability of 2D CCP-1 and 2D CCP-2 were further investigated under UV irradiation for two hours (**see SI for details**). After the UV irradiation, the 2D CCP-1 exhibits the PLQY of 21.6%, corresponding to 87% of the PLQY of the initial value. The PLQY of 2D CCP-2 still retains 32.3 %, same to the initial PLQY (**Figure 4b**). Here, for comparison, the well-known small molecular emitter tetrakis(carbazol-9-yl)-4,6-dicyanobenzene (4CzIPN) with C-N, C-C, and C-H bonds was chosen. The emitter 4CzIPN has been widely used and thoroughly studied for organic light-emitting diodes and bio-imaging.[10,25] As depicted in **Figure 4a**, the PLQY of 4CzIPN can only retain 43% of the initial value under the same UV irradiation conditions after two hours. The PXRD patterns of both 2D CCPs before and after UV irradiation suggest that both emissive 2D CCPs maintain high crystallinities (**Figure 4c**). Compared with 4CzIPN, these investigations demonstrate the excellent photostability for both CN-substituted 2D CCPs. The high photostability can be attributed to two reasons: (1) The 2D conjugated polymers with a rigid CN-substituted vinylene-linked skeleton can significantly reduce the photodegradation rates;[8,9] (2) In the stacking direction, according to the simulated models, the short distance between the C=C bonds of adjacent layers is about 6.2 and 6.0 Å for 2D CCP-1 and 2D CCP-2 (**Figure 4d**), respectively, which is clearly larger than 4.2 Å which is required for a possible interlayer [2+2] photocycloaddition between two C=C bonds.[8,30] Thus, the large interlayer distance manifests the weak π-π stacking between the layered structures of 2D CCPs, which can lead to enhanced solid-state emission.[2]

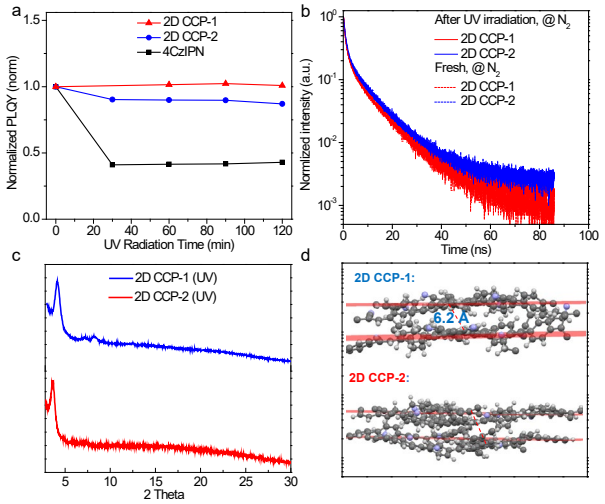

Figure 4. (a) Photostability investigation for the synthesized 2D CCP-1 (blue) and 2D CCP-2 (red), compared to the reported small molecular emitter 4CzIPN (black), in which the initial PLQY is normalized to one. (b) The luminescence decay of the 2D CCP-1 (blue) and 2D CCP-2 (red) before and after UV irradiation for two hours; (c) PXRD patterns of 2D CCP-1 (bue) and 2D CCP-2 (red) after UV irradiation for two hours; (d) Simulated distance between C=C bonds in adjacent crystalline layers of 2D CCP-1 (top) and 2D CCP-2 (down), where the red lines represent the crystal plane.

Conclusion

In summary, the chromophore triphenylene is incorporated into two robust CN-substituted 2D CCPs, namely phenylene-based 2D CCP-1 and biphenyl-based 2D CCP-2. Both 2D CCPs with dual pore structures are identified by IR spectroscopy, solid-state NMR measurements, PXRD studies, and N_2 adsorption-desorption measurements. Due to the twist and rigid nature of [-CH=C(CN)-] linkages, both 2D CCPs exhibit strong solid-state emission with absolute PLQY of up to 32.3%, which is a record value for the reported 2D conjugated polymers. Compared with a well-known organic emitter 4CzIPN, the robust skeleton of CN-substituted 2D CCPs renders high photostability for two hours under UV irradiation. This work enriches the structural diversity of CN-substituted 2D CCPs and also broadens the family of the stable emissive emitters based on metal-free organic composition. We anticipate that these highly luminescent 2D CCPs with high photostability can pave the way for future applications in optoelectronics, bio-imaging, and photocatalysis.

ASSOCIATED CONTENT

Supporting Information. The Supporting Information is available free of charge on the http://pubs.acs.orgat DOI: http://pubs.acs.org The Supporting Information include the synthesis of monomers and 2D conjugated polymers; FT-IR spectra; Solid-State ^{13}C NMR spectra, SEM images, TEM images, experimental and modeling PXRD, BET surface area plots, UV-Vis absorption spectroscopy, fluorescence emission spectroscopy; TCSPC data for the prompt emission; NMR spectra of the monomer HFPTP.

AUTHOR INFORMATION

Corresponding Author

E-mail: xinliang.feng@tu-dresden.de

E-mail: sebastian.reineke@tu-dresden.de

Author Contributions

All authors have given approval to the final version of the manuscript.

[#]These authors contributed equally.

ACKNOWLEDGMENT

We thank the financial support from the DFG for the CRC 1415 (No. 417590517), the ERC Consolidator Grant (T2DCP), Coordination Networks: Building Blocks for Functional Systems (SPP 1928, COORNET), EU Graphene Flagship (GrapheneCore3; No. 881603), H2020-MSCA-ITN (ULTIMATE, No. 813036), as well as the German Science Council and Center of Advancing Electronics Dresden (cfaed).We thank Dr. Philipp Schlender for PXRD measurements. We thank Dr. Petr Formanek (Leibniz Institute for Polymer Research, IPF, Dresden) for the TEM measurements.

REFERENCES

(1) Reineke, S.; Thomschke, M.; Lüssem, B.; Leo, K. White Organic Light-Emitting Diodes: Status and Perspective. *Rev. Mod. Phys.* **2013**, *85*, 1245–1293.

(2) Mei, J.; Leung, N. L. C.; Kwok, R. T. K.; Lam, J. W. Y.; Tang, B. Z. Aggregation-Induced Emission: Together We Shine, United We Soar! *Chem. Rev.* **2015**, *115*, 11718–11940.

(3) Hou, L.; Zhang, X.; Cotella, G. F.; Carnicella, G.; Herder, M.; Schmidt, B. M.; Pätzel, M.; Hecht, S.; Cacialli, F.; Samorì, P. Optically Switchable Organic Light-Emitting Transistors. *Nat. Nanotechnol.* **2019**, *14*, 347–353.

(4) Kuehne, A. J. C.; Gather, M. C. Organic Lasers: Recent Developments on Materials, Device Geometries, and Fabrication Techniques. *Chem. Rev.* **2016**, *116*, 12823–12864.

(5) Shamsi, J.; Urban, A. S.; Imran, M.; De Trizio, L.; Manna, L. Metal Halide Perovskite Nanocrystals: Synthesis, Post-Synthesis Modifications, and Their Optical Properties. *Chem. Rev.* **2019**, *119*, 3296–3348.

(6) Reineke, S.; Lindner, F.; Schwartz, G.; Seidler, N.; Walzer, K.; Lüssem, B.; Leo, K. White Organic Light-Emitting Diodes with Fluorescent Tube Efficiency. *Nature* **2009**, *459*, 234–238.

(7) Li, Y.; Kovačič, M.; Westphalen, J.; Oswald, S.; Ma, Z.; Hänisch, C.; Will, P. A.; Jiang, L.; Junghaehnel, M.; Scholz, R.; Lenk, S.; Reineke, S. Tailor-Made Nanostructures Bridging Chaos and Order for Highly Efficient White Organic Light-Emitting Diodes. *Nat. Commun.* **2019**, *10*, 2972.

(8) Shahid, I. *Failure Analysis of Tools*; 2004; Vol. 162.

(9) Lin, N.; Qiao, J.; Duan, L.; Wang, L.; Qiu, Y. Molecular Understanding of the Chemical Stability of Organic Materials for OLEDs: A Comparative Study on Sulfonyl, Phosphine-Oxide, and Carbonyl-Containing Host Materials. *J. Phys. Chem. C* **2014**, *118*, 7569–7578.

(10) Sandanayaka, A. S. D.; Matsushima, T.; Adachi, C. Degradation Mechanisms of Organic Light-Emitting Diodes Based on Thermally Activated Delayed Fluorescence Molecules. *J. Phys. Chem. C* **2015**, *119*, 23845–23851.

(11) Chen, X.; Geng, K.; Liu, R.; Tan, K. T.; Gong, Y.; Li, Z.; Tao, S.; Jiang, Q.; Jiang, D. Covalent Organic Frameworks: Chemical Approaches to Designer Structures and Built-In Functions. *Angew. Chem. Int. Ed.* **2020**, *59*, 5050–5091.

(12) Li, X.; Yadav, P.; Loh, K. P. Function-Oriented Synthesis of Two-Dimensional (2D) Covalent Organic Frameworks – from 3D Solids to 2D Sheets. *Chem. Soc. Rev*., **2020**, *49*, 4835-4866.

(13) Mahmood, J.; Lee, E. K.; Jung, M.; Shin, D.; Jeon, I. Y.; Jung, S. M.; Choi, H. J.; Seo, J. M.; Bae, S. Y.; Sohn, S. D.; Park, N.; Oh, J. H.; Shin, H. J.; Baek, J. B. Nitrogenated Holey Two-Dimensional Structures. *Nat. Commun.* **2015**, *6*, 6486.

(14) Kim, S. J.; Mahmood, J.; Kim, C.; Han, G. F.; Kim, S. W.; Jung, S. M.; Zhu, G.; De Yoreo, J. J.; Kim, G.; Baek, J. B. Defect-Free Encapsulation of Fe0 in 2D Fused Organic Networks as a Durable Oxygen Reduction Electrocatalyst. *J. Am. Chem. Soc.* **2018**, *140*, 1737–1742.

(15) Marco, A. B.; Cortizo-Lacalle, D.; Perez-Miqueo, I.; Valenti, G.; Boni, A.; Plas, J.; Strutyński, K.; De Feyter, S.; Paolucci, F.; Montes, M.; Khlobystov, A. N.; Melle-Franco, M.; Mateo-Alonso, A. Twisted Aromatic Frameworks: Readily Exfoliable and Solution-Processable Two-Dimensional Conjugated Microporous Polymers. *Angew. Chem. Int. Ed.* **2017**, *56*, 6946–6951.

(16) Li, X.; Gao, Q.; Wang, J.; Chen, Y.; Chen, Z. H.; Xu, H. S.; Tang, W.; Leng, K.; Ning, G.-H.; Wu, J.; Xu, Q.-H.; Quek, S. Y.; Lu, Y.; Loh, K. P. Tuneable near White-Emissive Two-Dimensional Covalent Organic Frameworks. *Nat. Commun.* **2018**, *9*, 2335.

(17) Caruso, U.; Panunzi, B.; Diana, R.; Concilio, S.; Sessa, L.; Shikler, R.; Nabha, S.; Tuzi, A.; Piotto, S. AIE/ACQ Effects in Two DR/NIR Emitters: A Structural and DFT Comparative Analysis. *Molecules* **2018**, *23*, 1947.

(18) Jin, E.; Li, J.; Geng, K.; Jiang, Q.; Xu, H.; Xu, Q.; Jiang, D. Designed Synthesis of Stable Light-Emitting Two-Dimensional Sp^2 Carbon-Conjugated Covalent Organic Frameworks. *Nat. Commun.* **2018**, *9*, 4143.

(19) Becker, D.; Biswal, B. P.; Kaleńczuk, P.; Chandrasekhar, N.; Giebeler, L.; Addicoat, M.; Paasch, S.; Brunner, E.; Leo, K.; Dianat, A.; Cuniberti, G.; Berger, R.; Feng, X. Fully Sp^2 -Carbon-Linked Crystalline Two-Dimensional Conjugated Polymers: Insight into 2D Poly(Phenylenecyanovinylene) Formation and Its Optoelectronic Properties. *Chem. Eur. J.* **2019**, *25*, 6562–6568.

(20) Ding, S. Y.; Dong, M.; Wang, Y. W.; Chen, Y. T.; Wang, H. Z.; Su, C. Y.; Wang, W.; Thioether-Based Fluorescent Covalent Organic Framework for Selective Detection and Facile Removal of Mercury(II). *J. Am. Chem. Soc.* **2016**, *138*, 3031–3037.

(21) Haldar, S.; Chakraborty, D.; Roy, B.; Banappanavar, G.; Rinku, K.; Mullangi, D.; Hazra, P.; Kabra, D.; Vaidhyanathan, R. Anthracene-Resorcinol Derived Covalent Organic Framework as Flexible White Light Emitter. *J. Am. Chem. Soc.* **2018**, *140*, 13367–13374.

(22) Albacete, P.; Martínez, J. I.; Li, X.; López-Moreno, A.; Mena-Hernando, S.; Platero-Prats, A. E.; Montoro, C.; Loh, K. P.; Pérez, E. M.; Zamora, F. Layer-Stacking-Driven Fluorescence in a Two-Dimensional Imine-Linked Covalent Organic Framework. *J. Am. Chem. Soc.* **2018**, *140*, 12922–12929.

(23) Li, Z.; Huang, N.; Lee, K. H.; Feng, Y.; Tao, S.; Jiang, Q.; Nagao, Y.; Irle, S.; Jiang, D. Light-Emitting Covalent Organic Frameworks: Fluorescence Improving via Pinpoint Surgery and Selective Switch-On Sensing of Anions. *J. Am. Chem. Soc.* **2018**, *140*, 12374–12377.

(24) Li, Z.; Zhang, Y.; Xia, H.; Mu, Y.; Liu, X. A Robust and Luminescent Covalent Organic Framework as a Highly Sensitive and Selective Sensor for the Detection of Cu^{2+} ions. *Chem. Commun.* **2016**, *52*, 6613–6616.

(25) Uoyama, H.; Goushi, K.; Shizu, K.; Nomura, H.; Adachi, C. Highly Efficient Organic Light-Emitting Diodes from Delayed Fluorescence. *Nature* **2012**, *492*, 234–238.

(26) Xu, S.; Wang, G.; Biswal, B. P.; Addicoat, M.; Paasch, S.; Sheng, W.; Zhuang, X.; Brunner, E.; Heine, T.; Berger, R.; Feng, X. A Nitrogen-Rich 2D Sp^2-Carbon-Linked Conjugated Polymer Framework as a High-Performance Cathode for Lithium-Ion Batteries. *Angew. Chem. Int. Ed.* **2019**, *58*, 849–853.

(27) Rüger, R.; Van Lenthe, E.; Heine, T.; Visscher, L. Tight-Binding Approximations to Time-Dependent Density Functional Theory - A Fast Approach for the Calculation of Electronically Excited States. *J. Chem. Phys.* **2016**, *144*, 184103.

(28) Fries, F.; Reineke, S. Statistical Treatment of Photoluminescence Quantum Yield Measurements. *Sci. Rep.* **2019**, *9*, 15638.

(29) Rörich, I.; Schönbein, A. K.; Mangalore, D. K.; Halda Ribeiro, A.; Kasparek, C.; Bauer, C.; Crăciun, N. I.; Blom, P. W. M.; Ramanan, C. Temperature Dependence of the Photo- and Electroluminescence of Poly(p-Phenylene Vinylene) Based Polymers. *J. Mater. Chem. C* **2018**, *6*, 10569–10579.

(30) Jadhav, T.; Fang, Y.; Liu, C.-H.; Dadvand, A.; Hamzehpoor, E.; Patterson, W.; Jonderian, A.; Stein, R. S.; Perepichka, D. F. Transformation between 2D and 3D Covalent Organic Frameworks via Reversible [2 + 2] Cycloaddition. *J. Am. Chem. Soc.* **2020**, *142*, 8862–8870.

(31) Fries, F.; Reineke, S. Statistical treatment of Photoluminescence Quantum Yield Measurements. *Sci. Rep*. **2019**, *9*, 15638.

(32) Li, Y.; Wei, Q.; Cao, L.; Fries, F.; Cucchi, M.; Wu, Z.; Scholz, R.; Lenk, S.; Voit, B.; Ge, Z.; Reineke, S. Organic Light-Emitting Diodes Based on Conjugation-Induced Thermally Activated Delayed Fluorescence Polymers: Interplay Between Intra- and Intermolecular Charge Transfer States. *Front. Chem*. **2019**, *7*, 688.

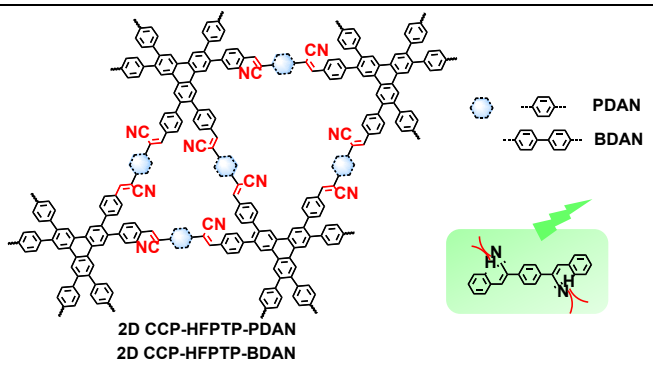

Two-dimensional sp^2-Carbon-Linked Conjugated Polymers (2D CCPs) with High Luminescence and Photostability